Materials Today Energy 14 (2019) 100350

Contents lists available at ScienceDirect

Materials Today Energy

journal homepage: www.journals.elsevier.com/materials-today-energy/

Giant bulk photovoltaic effect in solar cell architectures with ultra-wide bandgap Ga_2O_3 transparent conducting electrodes

A. Pérez-Tomás [a, *], E. Chikoidze [b], Y. Dumont [b], M.R. Jennings [c, d], S.O. Russell [c], P. Vales-Castro [a], G. Catalan [a, e], M. Lira-Cantú [a], C. Ton –That [f], F.H. Teherani [g], V.E. Sandana [g], P. Bove [g], D.J. Rogers [g]

[a] Catalan Institute of Nanoscience and Nanotechnology (ICN2), CSIC and BIST, Campus UAB, Bellaterra, 08193 Barcelona, Spain
[b] Groupe D'Etude de La Matière Condensee (GEMaC), Université de Versailles Saint Quentin en Y. - CNRS, Université Paris-Saclay, 45 Av. des Etats-Unis, 78035, Versailles Cedex, France
[c] Faculty of Science, University of Warwick, Coventry, CV4 7AL, UK
[d] Swansea University, Bay Campus, Fabian Way, Crymlyn Burrows, Swansea, SA1 8EN, UK
[e] Institut Català de Recerca I Estudis Avançats (ICREA), Barcelona, 08010, Catalonia, Spain
[f] School of Mathematical and Physical Science, University of Technology Sydney, Broadway, PO Box 123, NSW, 2007, Australia
[g] Nanovation, 8 Route de Chevreuse, 78117, Châteaufort, France

ARTICLE INFO

Article history:
Received 1 July 2019
Received in revised form
20 August 2019
Accepted 16 September 2019
Available online 7 October 2019

Keywords:
Ultra-wide bandgap semiconductors
Transparent conducting oxide
Gallium oxide
Ga_2O_3
Ferroelectric photovoltaics
$Pb(Zr,Ti)O_3$
Bulk photovoltaic effect
Solar cell architecture

ABSTRACT

The use of ultra-wide bandgap transparent conducting beta gallium oxide (β-Ga_2O_3) thin films as electrodes in ferroelectric solar cells is reported. In a new material structure for energy applications, we report a solar cell structure (a light absorber sandwiched in between two electrodes - one of them - transparent) which is not constrained by the Shockley–Queisser limit for open-circuit voltage (V_{oc}) under typical indoor light. The solar blindness of the electrode enables a record-breaking bulk photovoltaic effect (BPE) with white light illumination (general use indoor light). This work opens up the perspective of ferroelectric photovoltaics which are not subject to the Shockley-Queisser limit by bringing into scene solar-blind conducting oxides.

1. Introduction

A photovoltaic device generally requires at least one transparent conducting electrode for the light to reach the active light absorbing layers [1]. Although there has been recent interest in using correlated metals [2] and carbon-based materials such as graphene [3] transparent conducting metal oxides (TCO) based on degenerately doped In_2O_3, SnO_2 or ZnO and their alloys are currently the standard choice for transparent electrode applications [4–6]. These oxide semiconductors have bandgaps between about 3.1 and 3.7 eV, which make them "visible-blind" and suitable for applications requiring transmission up to the near-ultraviolet spectral range. Apart from being a fundamental element of a solar cell, such transparent electrodes are also hugely important for information and communication technologies such as displays, touch screens or light emitting diodes [7–9].

Amongst other semiconductor oxides, the monoclinic β-form of gallium oxide (β-Ga_2O_3) stands out because it has the widest band gap (~5 eV) among the practical TCOs and is transparent down to ~260 nm, enabling improved "solar blindness" in photonic and photovoltaic applications [10–12]. Furthermore, owing to its extreme bandgap, doping control and critical electric field (~8 MV/cm), ultra-wide bandgap Ga_2O_3 is the platform of choice for the emerging fourth generation of power electronic devices after silicon, silicon carbide and gallium nitride [13–15].

In parallel to the development of β-Ga_2O_3 as a TCO, and so far, completely independent of it, there is a growing interest in the bulk

* Corresponding author.
E-mail address: amador.perez@icn2.cat (A. Pérez-Tomás).

https://doi.org/10.1016/j.mtener.2019.100350
2468-6069/

photovoltaic effect (BPE) [16]. This effect allows homogeneous solids with a non-centrosymmetric lattice (i.e. piezoelectric, pyroelectric and ferroelectric materials) to develop a steady photovoltaic current even in the absence of chemical potential gradients [17]. Excitingly, and unlike the classical semiconductor-junction photovoltaic effect, the BPE is not subject to the Shockley-Queisser limit and it allows photovoltages much larger than the bandgap. Consequently, extremely large photoelectric fields of up to millions of Volts per centimeter can be expected [18]. Moreover, in the case of ferroelectrics, which are materials with persistent and switchable polarization, the sign and direction of BPE photovoltages and photocurrents may be inverted. Properly engineered, this kind of anomalous photovoltaic effect enables innovative energy conversion applications involving photons [19–21]. In practical devices, however, the photo-response should be generated by either the solar spectrum (outdoor natural sunlight) or indoor light (illumination without ultraviolet and infrared components), and therein lies a key issue: ferroelectrics that show above-bandgap photovoltages are generally wide-bandgap materials that only display a BPE response with illumination in the UV or near-UV range.

The recent approach to try to solve this problem has been to engineer ferroelectrics with a bandgap lying in the visible region in order to promote natural light harvesting [22–25]. Although Yang et al. [23] obtained visible anomalous photovoltaic effects in lateral structures (attributed to a domain wall tandem effect), the overwhelming majority of narrow-bandgap ferroelectric solar cells reported so far present disappointing photovoltages which are well below bandgap [26]. Crucially, no voltages greater than the bandgap have been reported in ferroelectric thin-film solar cells with conventional vertical structures (i.e. with a ferroelectric layer sandwiched between a top metallic electrode and a transparent superstrate electrode) -see Fig. 1-a, f - under solar/white illumination ([26] and references there in).

Here we show that adoption of β-Ga_2O_3 as the transparent electrode for BPE resolves this problem and allows a thin film solar cell with a conventional wide-bandgap ferroelectric (i.e. lead zirconate-titanate $PbZr_xTi_{1-x}O_3$ $x = 0.53$ or PZT) to display a giant BPE under white light. Therefore, with this approach we are able to break the S-Q limit for the maximum photovoltage in a sandwich-solar cell structure.

2. Giant BPE under white light illumination

In this experiment, model ferroelectric PZT thin-films were grown on both β-Ga_2O_3 (also labelled as GAO) and fluorine-doped tin oxide (FTO) (Fig. 1-a-d). The nominally undoped β-Ga_2O_3 epilayers were grown on r-sapphire substrates using pulsed laser-deposition. The thickness of the β-Ga_2O_3 was ~350 nm and the bandgap was ~5.2 eV. Its unique conducting 2D surface channel conductivity and carrier mobility were found to be 20 $\Omega^{-1}cm^{-1}$ and 6 cm^2/V, respectively [27], and it will be analyzed more in detail in the discussion section. FTO/glass was chosen as a reference electrode because it is widely used as a transparent conducting superstrate for third generation solar cells [28,29]. The thickness and conductivity of the FTO electrode were 80 nm and 1.4×10^4 $\Omega^{-1}cm^{-1}$, respectively.

The kinetic energy spectra (Fig. 1-e) for photoelectrons in the valence-band were determined by ultraviolet photoelectron spectroscopy (UPS) for both transparent electrodes (see methods). It was observed that the absorption bandgap tailed off significantly deeper in the ultraviolet for the β-Ga_2O_3 compared with the FTO. Fig. 1-c also shows the emission spectrum for a white light-emitting diode (LED), as determined by a spectrophotometer (see methods). It is noticeable the FTO absorption tail states overlap with the LED emission spectrum while there is no overlap for the β-Ga_2O_3 absorption tail states.

A top electrode of silver was evaporated on both structures so as to form a sandwiched photovoltaic cell, as shown in Fig. 2-a,b. The solution process (described in methods) involved spin-coating of a Pb–Zr–Ti solution on the transparent electrode and an anneal in the temperature range of 550–650 °C (Figs. S1–S3). X-ray diffraction revealed the PZT films to be pure perovskite with a pseudo-cubic lattice parameter $a = 4.077$ Å, for both types of electrode (Fig. 2). The thickness of the PZT layers was ~90 nm (see methods). The optical bandgap of PZT was determined to be 3.6 eV using a Tauc plot, as described in methods (Fig. S4). Therefore, the PZT layer is indeed a wide-bandgap semiconductor where, in principle, photo-carriers could only be photo-excited under white LED illumination via absorption tail states that extend into the visible spectrum (Figs. S5–S7). Ferroelectric characterization via hysteresis loops (see Fig. 2-f) revealed large remnant (20 $\mu C/cm^2$) and saturation (40 $\mu C/cm^2$) polarization in the PZT.

Photovoltaic characterization was performed by current-voltage recording under illumination as described in methods. Ferroelectric poling was accomplished through a series of consecutive monopolar hysteresis loopings. A strikingly different photovoltaic behavior was observed for PZT/β-Ga_2O_3 compared to PZT/FTO, as shown in Fig. 3. While for PZT/β-Ga_2O_3 photo-current (j_{sc}) and photo-voltages (V_{oc}) could be reversed by inverting the polarization, such a behavior was not observed for PZT/FTO. Importantly, the photovoltage was above bandgap for the PZT/β-Ga_2O_3 (Fig. 3-b), but well below bandgap for the PZT/FTO, which had a V_{oc} smaller than 0.7 V. The above-bandgap photovoltages and their switchability for the PZT cells on β-Ga_2O_3 are both consistent with a BPE. In contrast, PZT/FTO did not show any sign of BPE (neither switching of photocurrent sign nor above-bandgap voltage) even after intensive testing of alternative poling routes or changing the PZT growth parameters (Figs. S9 and S10). The breaking-record maximum measured photovoltage for PZT/β-Ga_2O_3 was 6.6 V (Fig. 1-f), which translated into very large photovoltaic fields (E_{pv}) of 0.7 MV/cm. As far as we know, this is the largest photovoltaic field observed for a ferroelectric under white light [30] and only second to antiferroelectric $PbZrO_3$ under UV-light [26] (and references there in).

3. Discussion

3.1. A unique Ga_2O_3 transparent conducting electrode

The origin of this enhanced photovoltaic behavior with β-Ga_2O_3 electrodes are a combination of the solar blindness and the relatively low density of defect states in the gap due to the epitaxial and undoped ,(*topological-like*") nature of the β-Ga_2O_3 film grown on r-sapphire. Here, the Ga_2O_3 transparent electrode is, in fact, the analogy of an extremely stable topological-like ultra-wide bandgap insulator, a solid that is a pure insulator in its bulk but has a metallic conductive surface. That conductive surface, in turn, was determined to be a two-dimensional conductive channel at the surface's vicinity [27]. The nominally undoped epitaxial β-Ga_2O_3 thin films without any detectable defect showed the unexpectedly low resistivity of ρ ~3×10^{-2} Ωcm which was found to be also resistant to high dose proton irradiation (2 MeV, $5 \times 10^{15} cm^{-2}$ dose) and was largely invariant (metallic) over the wide temperature range of 2 K up to 850 K. This high temperature stability is notable when compared with other correlated oxide systems such as confined 2D electrons at the metallic interface in between $LaAlO_3$ and $SrTiO_3$ [31] or in other oxide surfaces such as In_2O_3, ZnO, TiO_2, $BaTiO_3$, $SrTiO_3$ and $CaTiO_3$ (and non-oxides e.g. InN). These oxides have also been reported to host a surface two

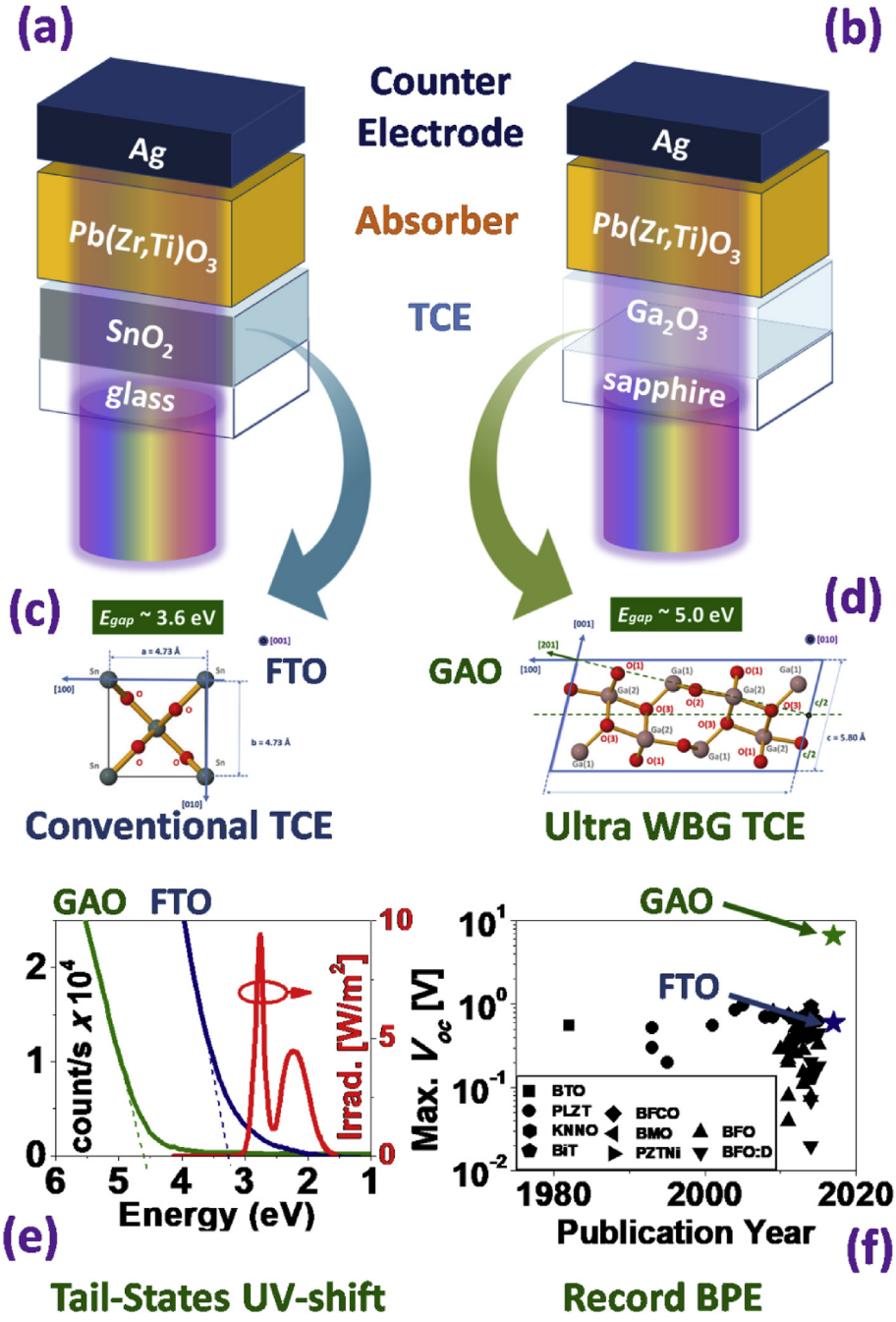

Fig. 1. (a),(b) Schematic of the sandwiched structure of the archetypical thin-film solar cell; i.e. transparent substrate/transparent conducting electrode (TCE)/active layers – absorber/metallic counter-electrode. Schematic of the investigated TCEs; (c) conventional FTO (or F:SnO_2)/glass vs. ultra-wide bandgap (d) GAO (or β-Ga_2O_3)/r-sapphire transparent electrodes. Note that the optical bandgap of the sapphire substrate (Al_2O_3) is even larger (~8 eV) than the one of Ga_2O_3. (e) Ultraviolet electron spectroscopy (UPS) results showing that the GAO tail states lie deeper in the ultraviolet such that the GAO spectrum shows almost no overlap with that of the white light-emitting diode (LED). (f) The ultra-wide bandgap GAO electrode allows breaking the Shockley–Queisser limit for open-circuit voltages with thin-film ferroelectric solar cell vertical architectures while the conventional FTO electrode results in similar performances to previous reports (data taken from the exhaustive survey in Ref.[26]).

dimensional electron gas but presenting however air instabilities and, in general, practical electrical conduction only at very low temperature (i.e., <100 K) [32]. Therefore, the degree of novelty of this study is notable; not only is the first time Ga_2O_3 is used as a transparent conducting electrode within a (ferroelectric) solar cell architecture but this investigation represents, as far as we know, the first time a surface oxide's 2D conductive channel has also been implemented in photovoltaics.

The origin of our Ga_2O_3 surface 2D conducting channel is still unclear. A number of high resolution techniques (including X-ray photoemission spectroscopy (XPS), energy dispersive X-ray spectroscopy (EDS), secondary ion mass spectroscopy (SIMS), Rutherford backscattering spectrometry (RBS) and depth-resolved cathode-luminescence (CL)) did not reveal any bulk or shallow donor signatures that could explain the conductivity in terms of conventional impurity or defect doping. In the literature, a very

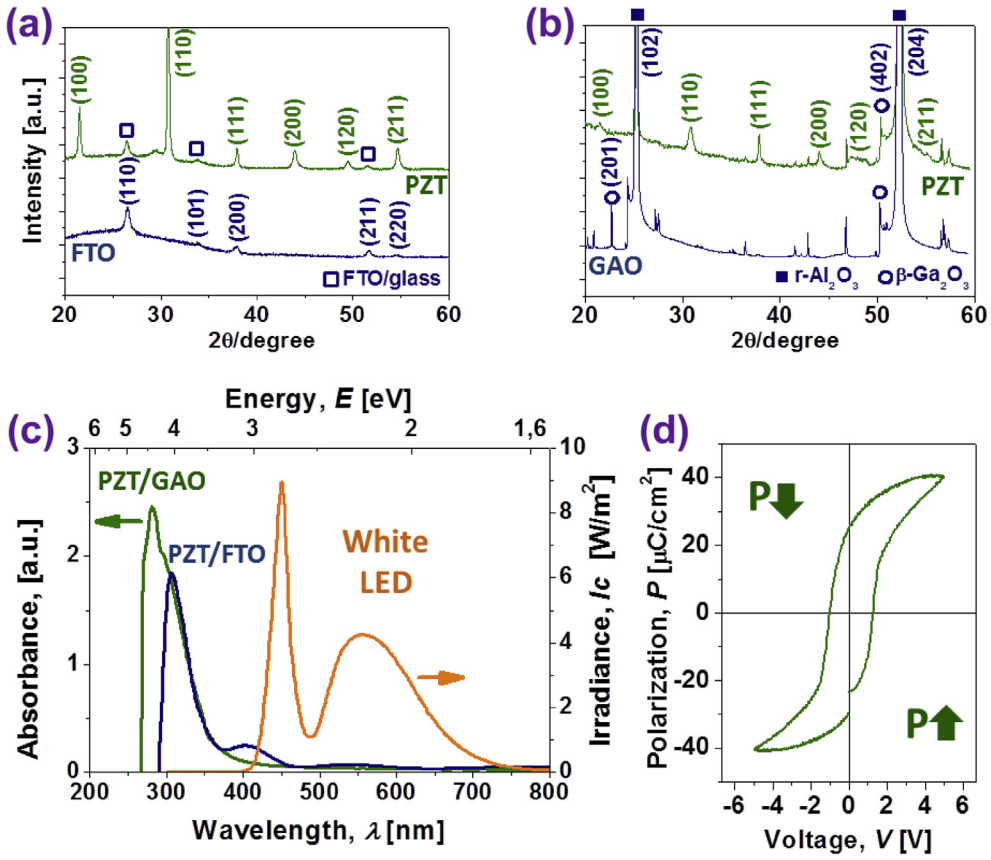

Fig. 2. X-ray diffraction scans revealing the same perovskite tetragonal phase (Pm-3m (211) space group) for the PZT grown on (a) FTO/glass and (b) the ultra-wide bandgap β-Ga_2O_3. (c) The UV–Vis spectra of the PZT/FTO and PZT/β-Ga_2O_3 structures showing both, the deeper ultraviolet cut-off and reduced absorbance in the visible range for PZT/β-Ga_2O_3. The white LED irradiance is superimposed. (d) Ferroelectric oxide layers exhibit large remnant polarization.

different nature of the bonding of interstitial hydrogen (H_i) in Ga_2O_3 compared to most other metal oxides has been suggested [33]. H_i has been suggested to act exclusively as shallow donors in Ga_2O_3 from theory and studies of the electronic analog muonium [34,35]. The bonding environment of the O atoms in Ga_2O_3 results in O lone-pairs that may capture H_i and form favorable shallow donors without much influence on the lattice, a phenomenon also exhibited by SnO_2. Hydrogen is perhaps the only element that cannot be directly detected by XPS. In the experiment of Swallow et al. [33], the surface of an as-entered (−201) Sn-doped (6×10^{18} cm^{-3}) Ga_2O_3 crystal (from Novel Crystal Technology, Inc., Tamura Corporation) was indirectly found to be terminated by O–H groups, resulting in downward band bending of 0.24 eV and electron accumulation with a sheet density of ~5×10^{12} cm^{-2}. Their XPS O1s peak main component was associated with O bonded to Ga at 532.2 eV while a shoulder component (1.3 eV higher in binding energy), was associated with a hydroxyl (−OH) group. According to the authors, this is likely due to H-adatoms bonding to O atoms on the Ga_2O_3 surface (surface adsorbates donate electrons into the surface accumulation layer [36]). Subsequent annealing (200–800 °C) reduces and eventually removes the shoulder component completely together with a O1s binding energy shift of ~0.7 eV to lower energy (531.6 eV). In our case, the 2D free electron concentration density profile for an undoped PLD thin-film (201) Ga_2O_3 epitaxial on sapphire was estimated by the Thomas–Fermi approximation for a 2D system to be as high as n_s ~2×10^{14} cm^{-2}. However, an analogous indirect analysis of the −OH groups by the O1s XPS peak shift has been determined to be smaller (~0.2 eV) [27]. (Surface) oxygen vacancies are other usual suspects for explaining the origin of oxide's surface 2DEG due to local chemical doping (see e.g. Refs. [37–41]). Although there are many conflicting reports on the shallow versus deep nature of its related electronic states, oxygen vacancies would form well-localized, compact donors but this fact does not preclude the possibility of these states being shallow in nature, by considering the energetic balance between the vacancy binding electrons that are in localized orbitals or in effective-mass-like diffuse orbitals [42].

In contrast, commercial TCOs, such as FTO, have non-negligible absorption in the visible owing to their smaller bandgap and the existence of significant sub-bandgap transitions due to doping/defect-related states in the gap [43]. This is a problem for the BPE because the surplus of carriers that this absorption generates is injected into the ferroelectric (as depicted in Fig. 3 c-d), resulting in interfacial carrier injection that cancel out the BPE current [44]. In non-centrosymmetric materials, light quanta absorption provides an asymmetric energy distribution of non-thermalized photo-generated carriers. These photo-carriers lose their energy in descending to the bottom of the conduction band, which generates a shift in k space and a BPE current [21]. The photo-carriers are further transported to the external connections by their respective TCOs, as depicted by their experimentally determined bandgap alignments (Fig. 3 c-d). While, for conventional photovoltaics additional TCO visible transitions are not a problem, they are a killer for the bulk photovoltaic effect for which any source of extrinsic conductivity is detrimental [17]. Whether a conventional degenerately doped Ga_2O_3 TCO would preserve a gigantic bulk photovoltaic effect is yet to be determined. In this sense, Peelaers et al. [45] have already reported (by hybrid density functional theory)

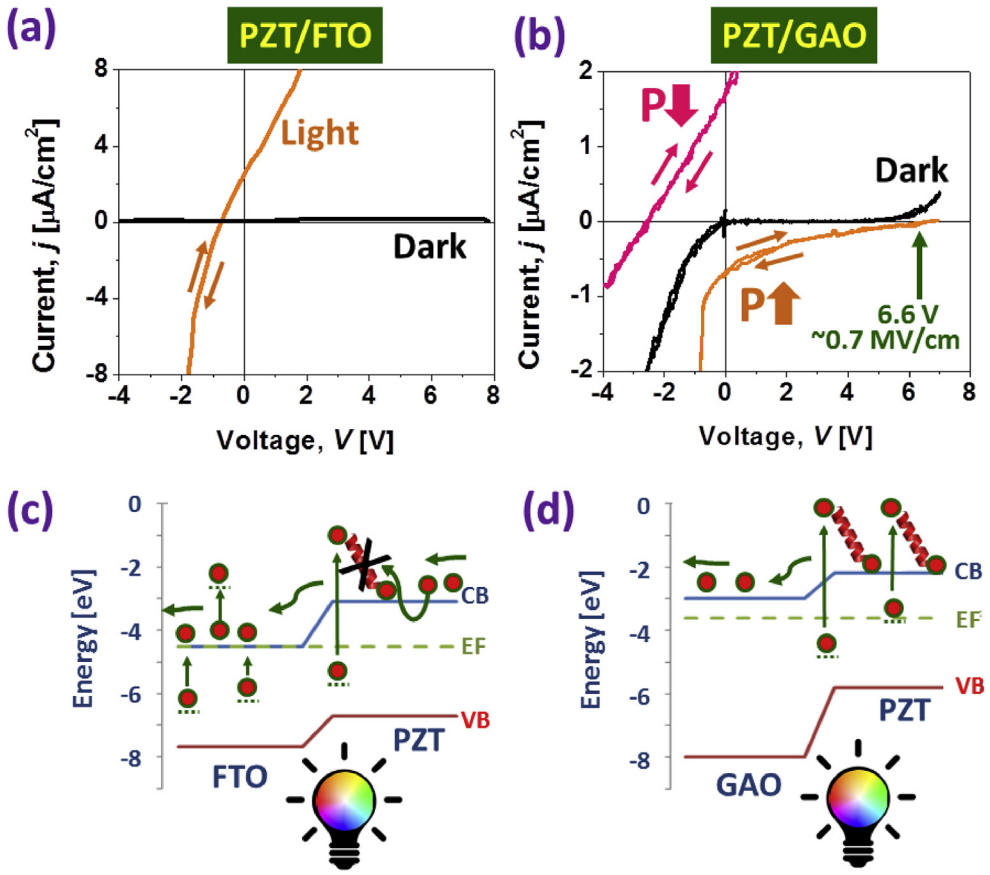

Fig. 3. (a) The PZT/FTO only exhibited a *conventional* photovoltaic effect signature in all cases with a photovoltage value (and sign) that did not depend on the polarization state and was always well below the PZT bandgap. (b) In contrast, above bandgap voltages were obtained for PZT/β-Ga_2O_3 with photovoltages and photocurrents that were switchable via hysteresis loop poling. The large photovoltaic field associated with the V_{oc} (6.6 V) of 0.7 MV/cm is generated with white-LED illumination. (c)–(d) β-Ga_2O_3's wider bandgap and lower sub-bandgap absorption suppress both the TCO charge injection and the scattering event rates and thus provide the conditions required for the emergence of the BPE produced by white light. The experimental band structure was determined by UPS/UV–Vis (see methods).

sub-band-gap absorption bands when increasing the doping on Ga_2O_3 above 10^{19} cm^{-3} owing to the enhancement of free carrier absorption (which also strongly depends on the polarization of the incoming light).

3.2. A bulk photovoltaic effect model

While there are theories about the origin of the bulk photovoltaic currents (in particular the so-called shift-current [46–48]), an accepted theory for the origin (and its related maximum magnitude) of the associated photovoltaic field is still missing (see e.g. Ref. [16]). This may be due to the fact that shift-currents are (somehow and sometimes) well explained by intrinsic phenomena (e.g. well-understood semiconductor band-to-band optical excitations) while their associated fields may be limited by a range of extrinsic effects such as lattice defects, dopants, interfacial barriers or the screening of the material's polarization. To make things more complex, many of these defects (if not all) introduce levels within the absorber bandgap that may be photo-excited with a particular light energy (i.e., wavelength), a phenomena that sometimes is referred under the umbrella of photorefraction. The illumination wavelength is therefore critically important; while bulk photovoltaic effects are relatively common under near ultraviolet light (see e.g. the review in Ref. [26]) there are, to the best of the author knowledge, no demonstration in sandwiched photovoltaic structures under broad wavelength illumination such as white light or (simulated) sun light. A part of the absorber's extrinsic defects/interfaces and the illumination spectra, the electrodes has a role. The observation of the electrodes affecting a ferroelectric photovoltaic device is indeed a very well-known effect (see e.g. Refs. [49,50]). For any photovoltaic device in general the choice of the electrodes (and/or buffer contact-layers) is critically important (the literature on this topic is huge - see e.g. Ref. [51] for a review for transparent conducting oxides and oxide buffers). So far, a change of electrodes in thin-film ferroelectric photovoltaic devices has been correlated with improvements in either photo-current or photo-voltage (or both). Typically, in these arrangements, such differences are explained in terms of modification of the Schottky barriers. Here, the changes in the photovoltage (more than 6 V) are simply too big to use conventional metal-semiconductor models. Besides, the photo-field of 0.7 MV/cm is much larger than any typical Schottky and *p-n* junction related space-charge field (typically ~10–100 kV). A tandem effect model does not hold. Notably, there is no appreciable developing photo-field characteristic time [18]. A photovoltaic developing time (in the range of few seconds to hours) is a typical signature of (near ultraviolet light) bulk photovoltaic effects [17] and, in turn, suggest a link with ionic drift, charge accumulation and polarization (switching) suppression [52–54]. If the photo-field upper bound is related with a pinned ferroic polarization, (the so-called Micheron criterion [55]), it would produce several MV/cm and ~100 V for a ~100 nm-thick layer, as already demonstrated in $PbZrO_3$ under near UV light [18]. If one assumes that the white light illumination is unable to produce structural polarization pining (or it has a much less *actinic* effect), it

is plausible to suggest that the experimental value of the photovoltage is determined by the amount of the ferroelectric polarization screening by photo-currents.

The experimental observation points out to the fact that the amount of screening is smaller with our undoped *topological-like* ultra-wide β-Ga_2O_3 electrodes [27] when compared to degenerately doped conventional transparent conducting oxides and, hence, the attainable open-circuit voltages much larger. From the Ga_2O_3/Pb(Zr,Ti)O_3 hysteresis loops we don't see an appreciable amount of imprint (internal fields affecting the ferroelectric's coercive field). The coercive field of our Pb(Zr,Ti)O_3 layers are typically ~50 kV/cm, one order of magnitude smaller than the experimental photovoltaic field. Therefore, we might say that a local electric field due to the Ga_2O_3 metallic surface would be too small to explain the photovoltaic field. Other incongruence lies in the fact that the photovoltaic field is switchable; the Ga_2O_3 layer conductivity (or its surface band bending) cannot be varied after an electric field. Thus, we have no indication of imprint in the ferroelectric that may explain the differences in the photocurrent and photovoltage behavior but an often overlooked property of ferroelectrics is that a polarization switch implies a switch in the surface band bending.

In traditional solid-state devices with *classic* semiconductors (e.g. Si and SiC), their electrical behavior is strongly dependent on the size of various band offsets and Schottky barriers in the junctions of differing material (e.g. Refs. [56,57]). Owing to its ultra-wide bandgap, the band-offset in between Ga_2O_3 and Pb(Zr,Ti)O_3 would be smaller than the band-offset in between SnO_2 and Pb(Zr,Ti)O_3 (Fig. 3 (c) and (d)) but these contact barriers and offsets may dramatically change depending on the ferroelectric polarization. It is well-known that chemical and structural factors can alter transition-metal oxide work functions. In particular, the ferroelectric photovoltaic phenomena would represent the kind of system where surface electric dipoles, absorbants and surface band bending play a major role [58–60]. It is also very well-known that the engineering of any metal-oxide work function within a solar cell architecture would show a direct correlation with the solar cell performance (e.g. Ref. [61]). In thin-film photovoltaics, in general, the low doped (intrinsic) absorber or the barrier extraction layers (either *n*-type or *p*-type) conductivities do not change. Either, a *n*-i-*p* or *p*-i-*n* configuration establishes the direction of the photocurrent by engineering the band-offset alignment [51]. The photocurrent flows to the outer electrodes when electrons shift to lower energies while the holes shift to higher energies (respect to the vacuum level). In the bulk photovoltaic effect with Ga_2O_3 transparent conducting electrodes reported here, the band bending of the Pb(Zr,Ti)O_3 interfaces may be reversed by an external electric field so that a switchable photocurrent may still be impressed which direction depends on the ferroelectric polarization (Fig. 4) [44]. This effect is lost when the ultra-wide bandgap Ga_2O_3 transparent conducting oxide (TCO) is replaced by a conventional TCO (SnO_2:F or FTO in this case), arguably because conventional highly doped TCOs aren't, indeed, totally transparent but they photogenerate parasitic carriers that effectively screens the absorber polarization. Here, we want to stress again that, for the Ga_2O_3 layer, a number of high resolution techniques (XPS, EDS, SIMS, RBS, CL) did not reveal any bulk or shallow donor signatures that could explain the conductivity in terms of conventional impurity or defect doping. Or in other words, it has been proven to be difficult to optically excite any "*impurity center*" in our *topological*-like Ga_2O_3, a kind of "*super-transparency*" so to speak.

In either case, there is no evidence of rectifying behavior at the interfaces [62]; we have not measured a single exponential J-V curve (dark or under illumination) but typically quadratic or linear J-V curves. Our FTO or GAO based solar cells aren't limited by a Schottky contact [63] but their transport mechanisms are rather

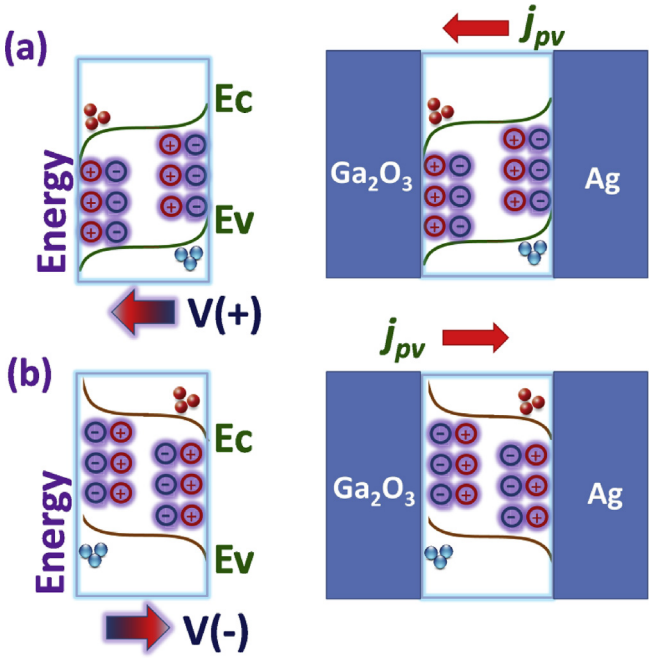

Fig. 4. Illustration of the switchable photocurrent direction and its relationship with the ferroelectric polarization induced band-bending for both, (a) *down* and (b) *up* ferroelectric polarization. The photo-current has been found to be non-limited by Schottky barriers (metal-semiconductor offsets) but following a bulk limited mechanism (i.e., space-charge current).

bulk limited [64]. Both metal electrodes may form Schottky interfaces to the PZT, especially if their work-functions vary depending on the ferroelectric polarization band-bending. However, if there is accumulation of charges at the interfaces, the Schottky depletion region is drastically thinned to the point to be in the tunneling contact regime (or field-emission) [65] and the absence of rectifying contacts is typical of the classic bulk photovoltaic effect. Indeed, the white LED photovoltaic curve is well fitted using a simple Moot-Gurney (also known as space-charge) transport law [66], $j = \widehat{V}(AV^2) - j_{pv}$, where $\widehat{V} = V/|V|$ and j_{pv} is the photovoltaic current. Either, in the low field limit and in the saturation regimen limit, the space charge current becomes linear with the field. The space charge limited transport is typical of sudden free-charge injection in insulators (in conducting solids the free charges are quickly neutralized, screened or drained) and therefore consistent with a bulk limited transport mechanism. A is a constant that has been found to be asymmetric depending on the polarity of the voltage, i.e., A^- and A^+ (see supplemental materials). The asymmetry is indeed usual in any non-ideal insulating thin-film; there is a frequent departure from the ideal law owing to defects and/or non-ideal injection regions [67]. The space-charge current asymmetry is also dependent on the effective dielectric constant (i.e., polarization variation with respect to an applied field) which is non-linear in ferroelectrics, assuming invariant electron mobility. It also further supports the hypothesis of the origin of the above bandgap voltages being unrelated to Schottky barriers or work functions but with a continuum of photo-generated space charges within the film. Even if an ad-hoc model is out of question, a qualitative expression can be derived taking into account the space charge hypothesis. In the open-circuit condition, $(AV^2) = j_{pv}$ or $(B\varepsilon V_{pv}^2) = j_{pv}$, where in the ideal case, the Mott-Gurney B constant is $B = 8\mu/9L^3$, ε is the dielectric constant, μ is the mobility and L is the slab thickness. The definition of the dielectric constant is $\varepsilon = 1 + \partial P/\partial E$ and in ferroelectrics ε is much larger than the unity

and therefore, $\varepsilon \approx \partial P/\partial E$. Thus, an expression can be derived for the open-circuit voltage as,

$$V_{pv} = \sqrt{\left(1 + \frac{\partial P}{\partial E}\right)^{-1}} \sqrt{\frac{j_{pv}}{B}} \quad (1)$$

Assuming that the second term $\sqrt{j_{pv}/B}$ is independent of the transparent conducting oxide acting as electrode, the space-charge photo-voltage depends on the amount of screening of the polarization or polarization pining. In the case of neutralizing charges being injected into the ferroelectric, the polarization is screened $(1 + \partial P/\partial E \approx 1)$ and the space-charge field remains low while if the polarization remains pinned a much larger photovoltage may be developed.

3.3. Future outlook

From a photovoltaic point of view, the most important result is that a giant BPE was obtained for a standard (wide-bandgap) ferroelectric under white light illumination (rather than with the near ultraviolet illumination that is generally required to produce a BPE in such ferroelectrics [18,30,68]). It is proposed that even bigger BPE currents could be possible by combining inorganic polar materials, such $LiAsSe_2$ [69], and organic compounds, such as conjugated vinylene-linked hybrid heterocyclic polymers [70], with solar blind transparent conducting electrodes to preserve the effect. Ga_2O_3 is a rising star amongst emerging ultra-wide bandgap semiconductors for solar blind transparent conducting electrodes [14]. Recently, Ga_2O_3 is receiving a lot of renewed attention as a transparent semiconducting oxide champion owing to its unusual material properties [71], large tuneable *n*-type and *p*-type conductivity [72], extremely high breakdown field [73] and the availability of high crystal quality at low cost wafers (6-inch) [74]. New opportunities will arise by exploiting the Ga_2O_3 ennabled bulk photovoltaic effect in innovative energy harvesting arrangements like sun-powered electronic converters [15] and buffering thin-film solar cells [75,76], solaristors [21] and water splitting systems [77].

4. Conclusions

Ferroelectric PZT/β-Ga_2O_3 exhibits BPE effects and switchable above-bandgap voltages under white LED illumination which were not observed for PZT/FTO reference samples. The record-breaking photovoltaic field (0.7 MV/cm) that was obtained represents a new landmark for ferroelectric thin-films and breaks the Shockley–Queisser limit for open-circuit voltages. It is proposed that this was enabled by the solar-blindness of β-Ga_2O_3 electrode, which facilitates activation of the absorption tail states of the ferroelectric without exciting neutralizing photo-carriers in the transparent electrode. Furthermore, the effect was engineered in straightforward vertical solar cell architectures based on transparent electrode superstrates. Although we are just at the beginning of the exploration of the transparent electrode potential of ultra-wide bandgap materials, the results presented in this letter already demonstrate that it may well open new territories for BPE based solar energy harvesting.

5. Experimental section

5.1. Ultra-wide bandgap β-Ga_2O_3 conductive epi

β-Ga_2O_3 layers (GAO) were grown on r-plane sapphire substrates by PLD from a commercial sintered 4N Ga_2O_3 target using a Coherent LPX KrF $\lambda = 248$ nm) laser. Uniform 2-inch diameter wafer coverage was obtained using optical rastering of the incident laser beam. Substrate temperature during growth was measured with a thermocouple to be ~550 °C and the ambient during growth was 10^{-4} torr of molecular oxygen. Ohmic contacts were done by indium-soldering. The resistivity and Hall Effect measurements were made by a physical property measurement system from Quantum Design USA using a specially designed (in home) Van der Pauw configuration. Further experimental details may be found in Ref. [27].

5.2. Ferroelectric thin-film definition

The synthesis of the PZT was done as follows: Zr-isopropoxide ($Zr[OCH(CH_3)_2]_4$ -70 wt % in 1-propanol- Sigma) and Ti-isopropoxide ($Ti[OCH\text{-}(CH_3)_2]_4$ (97%) Sigma) were mixed. Afterwards, acetic acid and *n*-propanol were added to the Zr/Ti solution. Then, Pb acetate (10% excess) [lead(II) acetate trihydrate, $Pb(CH_3CO_2)_2 \cdot 3H_2O$ (99.999%)] was dissolved into the above solution heating the solution in a silicon oil bath to 85 °C for dissolving the Pb precursor completely. After the cooling, down of the solution, acetic acid and distilled water were added to modify the Pb–Zr–Ti solution and adjust the solution to make 40 ml 0.4 M.

The GAO epitaxial TCO growth method is described in the previous section. The FTO substrates were bought from Solems, model ASAHI 100 by CVD of 1.1 mm thickness, (70-100-Ω resistance, thickness of FTO layer 800 Å.) were cleaned with soap water, mili-Q water, ethanol (99.5%) for 20 min before use. After an UV light cleaning step for 20 min, 80 μl of PZT solution was spin-coated on top of the GAO or FTO at 4000 rpm with an acceleration of 2000 rpm for 40s. The solution was dried in the hot plate for 5 min at 150 °C. The PZT layer was further annealed (400–650 °C) and/or oxidized (550–650 °C), for 10 min in air and/or 2 h in oxygen, respectively. Finally, a layer of 100 nm of the Ag metal was evaporated on top of the PZT layer in a BOC Edwards Auto 306 thermal evaporator. Devices were patterned using shadow masks with device area lying in the range of $3x10^{-4}$-0.2 cm^2.

5.3. Characterization

X-ray powder diffraction (XRD) analyses between 5 and 120° in a RIGAKU Rotaflex RU200 B instrument, using CuKα1 radiation.

X-ray photoelectron spectroscopy (XPS) and Ultraviolet photoelectron spectroscopy (UPS) measurements were performed with a Phoibos 150 analyzer (SPECS GmbH, Berlin, Germany)) in ultra-high vacuum conditions (base pressure 3 E-10 mbar). XPS measurements were performed with a monochromatic K alpha *x*-ray source (1486.74 eV) and UPS measurements were realized with monochromatic HeI UV source (21.2 eV). Work function determination was done by applying bias of −10 V at the sample.

Light-emitting diode (LED). The White-LED (W-LED) measurements were carried out in a home-made set-up attached to a probe station. The W-LED source is a commercial LED 3 × 1 W and 360 l m (lumens). The total irradiance has been determined to be $I = 888.9$ W m^{-2} and in the blue peak $I_{450} = 266.7$ W m^{-2}. I–V curves were measured with a Keithley model 6430 Sub-Femtoamp Remote SourceMeter.

Spectral Irradiance measurements were performed with a spectrophotometer SPECTRO 320 (D) release 5, 30932004, with gadget EOP-146 to measure the spectral irradiance. Spectral irradiance has been measured out-of-plane (90°) with a scan step of 1 nm and a speed of 100 ms/nm.

The UV–visible analysis of solutions and thin films were made in a Shimadzu 1800 spectrophotometer. The optical band gap was derived by the Tauc's relation; $\alpha h\nu = A(h\nu - E_g)^n$. Where, α is the absorbance, *A* is a constant, hν is photon energy, E_g is the allowed energy gap and $n = ½$ for allowed direct transitions. The PZT optical bandgap value was determined to be 3.6 eV.

The ferroelectric characterization was performed with a precision LC tester LCII Ferroelectric Test System unit of Radiant technologies attached to a probe station.

Acknowledgements

APT acknowledges Agencia Estatal de Investigación (AEI) and Fondo Europeo de Desarrollo Regional (FEDER) under contract ENE2015-74275-JIN. GC and PV also acknowledge financial support from the Generalitat de Catalunya (Grant 2017 SGR 579) and MINECO (National Plan MAT2016-77100-C2-1-P). The ICN2 is funded by the CERCA programme/Generalitat de Catalunya and by the Severo Ochoa programme of the Spanish Ministry of Economy, Industry and Competitiveness (MINECO, grant no. SEV-2017-0706). All authors acknowledge Dr G. Sauthier for the XPS/UPS measurements.

Appendix A. Supplementary data

Supplementary data to this article can be found online at https://doi.org/10.1016/j.mtener.2019.100350.

References

[1] D.S. Ginley, H. Hosono, D.C. Paine (Eds.), Handbook of Transparent Conductors, Springer, Golden, CO, USA, 2011.
[2] L. Zhang, Y. Zhou, L. Guo, W. Zhao, A. Barnes, H.-T. Zhang, C. Eaton, Y. Zheng, M. Brahlek, H.F. Haneef, N.J. Podraza, M.H.W. Chan, V. Gopalan, K.M. Rabe, R. Engel-Herbert, Correlated metals as transparent conductors, Nat. Mater. 15 (2016) 204–210.
[3] K.S. Kim, Y. Zhao, H. Jang, S.Y. Lee, J.M. Kim, K.S. Kim, J.-H. Ahn, P. Kim, J.-Y. Choi, B.H. Hong, Large-scale pattern growth of graphene films for stretchable transparent electrodes, Nature 457 (2009) 706–710.
[4] K. Ellmer, Past achievements and future challenges in the development of optically transparent electrodes, Nat. Photonics 6 (2012) 809–817.
[5] S.C. Dixon, D.O. Scanlon, C.J. Carmalt, I.P. Parkin, n-Type doped transparent conducting binary oxides: an overview, J. Mater. Chem. C 4 (2016) 6946–6961.
[6] K.H.L. Zhang, K. Xi, M.G. Blamire, R.G. Egdell, P-type transparent conducting oxides, J. Phys. Condens. Matter 28 (2016) 383002.
[7] X. Yu, T.J. Marks, A. Facchetti, Metal oxides for optoelectronic applications, Nat. Mater. 15 (2016) 383–396.
[8] K. Nomura, H. Ohta, A. Takagi, T. Kamiya, M. Hirano, H. Hosono, Room-temperature fabrication of transparent flexible thin-film transistors using amorphous oxide semiconductors, Nature 432 (2004) 488–492.
[9] F.P. García de Arquer, A. Armin, P. Meredith, E.H. Sargent, Solution-processed semiconductors for next-generation photodetectors, Nat. Rev. Mat. 2 (2017) 16100.
[10] M. Orita, H. Ohta, M. Hirano, H. Hosono, Deep-ultraviolet transparent conductive β-Ga_2O_3 thin films, Appl. Phys. Lett. 77 (2000) 4166.
[11] J. Kim, T. Sekiya, N. Miyokawa, N. Watanabe, K. Kimoto, K. Ide, Y. Toda, S. Ueda, N. Ohashi, H. Hiramatsu, H. Hosono, T. Kamiya, Conversion of an ultra-wide bandgap amorphous oxide insulator to a semiconductor, NPG Asia Mater. 9 (2017) e359.
[12] A. Pérez-Tomás, E. Chikoidze, M.R. Jennings, S.A.O. Russell, F.H. Teherani, P. Bove, E.V. Sandana, D.J. Rogers, Wide and ultra-wide bandgap oxides: where paradigm-shift photovoltaics meets transparent power electronics, in: Proc. SPIE 10533, Oxide-Based Materials and Devices IX, 6 March 2018, p. 105331Q. https://doi.org/10.1117/12.2302576.
[13] S.J. Pearton, J. Yang, P.H. Cary IV, F. Ren, J. Kim, M.J. Tadjer, M.A. Mastro, A review of Ga_2O_3 materials, processing, and devices, Appl. Phys. Rev. 5 (2018), 011301.
[14] J.Y. Tsao, S. Chowdhury, M.A. Hollis, et al., Ultrawide-bandgap semiconductors: research opportunities and challenges, Adv. Electron. Mater. 4 (2018) 1600501.
[15] E. Chikoidze, A. Fellous, A. Perez-Tomas, G. Sauthier, T. Tchelidze, C. Ton-That, T.T. Huynh, M. Phillips, S. Russell, M. Jennings, B. Berini, F. Jomard, Y. Dumont, P-type -gallium oxide: a new perspective for power and optoelectronic devices, Materials Today Physics 3 (2017) 118–126.
[16] L.Z. Tan, F. Zheng, S.M. Young, F. Wang, S. Liu, A.M. Rappe, Shift current bulk photovoltaic effect in polar materials-hybrid and oxide perovskites and beyond, npj Comput, Mater 2 (2016) 16026.
[17] P.J. Sturman, V.M. Fridkin, Photovoltaic and Photo-Refractive Effects in Non-centrosymmetric Materials, Gordon and Breach Science Publishers, 1992.
[18] A. Pérez-Tomás, M. Lira-Cantú, G. Catalan, Above-bandgap photovoltages in antiferroelectrics, Adv. Mater. 28 (2016) 9644.
[19] J.E. Spanier, V.M. Fridkin, A.M. Rappe, A.R. Akbashev, A. Polemi, Y. Qi, Z. Gu, S.M. Young, C.J. Hawley, D. Imbrenda, G. Xiao, A.L. Bennett-Jackson, C.L. Johnson, Power conversion efficiency exceeding the Shockley-Queisser limit in a ferroelectric insulator, Nat. Photonics 10 (2016) 611.
[20] L. Li, P.A. Salvador, G.S. Rohrer, Photocatalysts with internal electric fields, Nanoscale 6 (2014) 24.
[21] A. Pérez-Tomás, A. Lima, Q. Billon, I. Shirley, G. Catalán, M. Lira-Cantú, A solar transistor and photoferroelectric memory, Adv. Funct. Mater. 28 (2018) 1707099.
[22] T. Choi, S. Lee, Y.J. Choi, V. Kiryukhin, S.-W. Cheong, Switchable ferroelectric diode and photovoltaic effect in $BiFeO_3$, Science 324 (2009) 63.
[23] S.Y. Yang, J. Seidel, S.J. Byrnes, P. Shafer, C.H. Yang, M.D. Rossell, P. Yu, Y.H. Chu, J.F. Scott, J.W. Ager, Above-bandgap voltages from ferroelectric photovoltaic devices, Nat. Nanotechnol. 5 (2010) 143.
[24] I. Grinberg, D.V. West, M. Torres, G. Gou, D.M. Stein, L. Wu, G. Chen, E.M. Gallo, A.R. Akbashev, P.K. Davies, J.E. Spanier, A.M. Rappe, Perovskite oxides for visible-light-absorbing ferroelectric and photovoltaic materials, Nature 503 (2013) 509.
[25] R. Nechache, C. Harnagea, S. Li, L. Cardenas, W. Huang, J. Chakrabartty, F. Rosei, Bandgap tuning of multiferroic oxide solar cells, Nat. Photonics 9 (2015) 61.
[26] A. Pérez-Tomás, A. Mingorance, D. Tanenbaum, M. Lira-Cantú, Metal oxides in photovoltaics: all-oxide, ferroic, and perovskite solar cells [Ch. 8], in: The Future of Semiconductor Oxides in Next-Generation Solar Cells, Elsevier, Amsterdam, Netherlands, 2018, pp. 267–356. https://doi.org/10.1016/B978-0-12-811165-9.09989-0.
[27] E. Chikoidze, D.J. Rogers, F.H. Teherani, C. Rubio, G. Sauthier, H.J. Von Bardeleben, T. Tchelidze, C. Ton-That, A. Fellous, P. Bove, E.V. Sandana, Y. Dumont, A. Perez-Tomas, Puzzling robust 2D metallic conductivity in undoped β-Ga_2O_3 thin films, Materials Today Physics 8 (2019) 10–17.
[28] S.S. Shin, E.J. Yeom, W.S. Yang, S. Hur, M.G. Kim, J. Im, J. Seo, J.H. Noh, S.I. Seok, Colloidally prepared La-doped $BaSnO_3$ electrodes for efficient, photostable perovskite solar cells, Science (2017), https://doi.org/10.1126/science.aam6620.
[29] O. Ostroverkhova, Organic optoelectronic materials: mechanisms and applications, Chem. Rev. 116 (2016) 13279–13412.
[30] A. Zenkevich, Yu Matveyev, K. Maksimova, R. Gaynutdinov, A. Tolstikhina, V. Fridkin, Giant bulk photovoltaic effect in thin ferroelectric $BaTiO_3$ films, Phys. Rev. B 90 (2014) 161409(R).
[31] S.Y. Moon, ChW. Moon, H.J. Chang, T. Kim, Ch-Y. Kang, H.-J. Choi, J.-S. Kim, S. Hyub Baek, H.W. Jang, Thermal stability of 2DEG at amorphous $LaAlO_3$/crystalline $SrTiO_3$ heterointerfaces, Nano Convergence 12 (2016) 243.
[32] A.F. Santander-Syro, O. Copie, T. Kondo, F. Fortuna, S. Pailhès, R. Weht, X.G. Qiu, et al., Two-dimensional electron gas with universal subbands at the surface of $SrTiO_3$, Nature 469 (2011) 189.
[33] J.E.N. Swallow, J.B. Varley, L.A.H. Jones, J.T. Gibbon, L.F.J. Piper, V.R. Dhanak, T.D. Veal, Transition from electron accumulation to depletion at β-Ga2O3 surfaces: the role of hydrogen and the charge neutrality level, Apl. Mater. 7 (2019), 022528.
[34] J.B. Varley, J.R. Weber, A. Janotti, C.G. Van de Walle, Oxygen vacancies and donor impurities in β-Ga_2O_3, Appl. Phys. Lett. 97 (2010) 142106.
[35] P.D.C. King, I. McKenzie, T.D. Veal, Observation of shallow-donor muonium in Gashallow-donor muonium in Ga_2: Evidence for hydrogen-induced conductivity$_3$: Evidence for hydrogen-induced conductivity, Appl. Phys. Lett. 96 (2010), 062110.
[36] P.C.J. Clark, A.I. Williamson, N.K. Lewis, R. Ahumada-Lazo, M. Silly, J.J. Mudd, C.F. McConville, W.R. Flavell, Origin of the two-dimensional electron gas at the CdO (100) surface, Phys. Rev. B 99 (2019), 085433.
[37] S. Lany, A. Zakutayev, T.O. Mason, J.F. Wager, K.R. Poeppelmeier, J.D. Perkins, J.J. Berry, D.S. Ginley, A. Zunger, Surface Origin of high Conductivities in undoped In_2O_3 thin films, Phys. Rev. Lett. 108 (2012), 016802.
[38] T.C. Rödel, F. Fortuna, F. Bertran, M. Gabay, M.J. Rozenberg, A.F. Santander-Syro, P. Le Fèvre, Engineering two-dimensional electron gases at the (001) and (101) surfaces of TiOtwo-dimensional electron gases at the (001) and (101) surfaces of TiO_2 anatase using light, Phys. Rev. B 92 (2015), 041106.
[39] S. Muff, M. Fanciulli, A.P. Weber, N. Pilet, Z. Ristić, Z. Wang, N.C. Plumb, M. Radović, J. Hugo Dil, Observation of a two-dimensional electron gas at CaTiOtwo-dimensional electron gas at $CaTiO_3$ film surfaces, Appl. Surf. Sci. 432 (2018) 41–45. Part A.
[40] A. Walsh, Surface oxygen vacancy origin of electron accumulation in indium oxide, Appl. Phys. Lett. 98 (2011) 261910.
[41] E. Frantzeskakis, C.R. Tobias, F. Franck, S.-S. Andrés Felipe, 2D surprises at the surface of 3D materials: confined electron systems in transition metal oxides, J. Electron. Spectrosc. Relat. Phenom. 219 (2017) 16–28.
[42] J. Buckeridge, C.R.A. Catlow, M.R. Farrow, A.J. Logsdail, D.O. Scanlon, T.W. Keal, P. Sherwood, S.M. Woodley, A.A. Sokol, A. Walsh, Deep vs shallow nature of oxygen vacancies and consequent n-type carrier concentrations in transparent conducting oxides, Phys. Rev. Materials 2 (2018), 054604.
[43] C.D. Canestraro, M.M. Oliveira, R. Valaski, M.V.S. da Silva, D.G.F. David, I. Pepe, A.F. da Silva, L.S. Roman, C. Persson, Strong inter-conduction-band absorption in heavily fluorine doped tin oxide, Appl. Surf. Sci. 255 (2008) 1874–1879.
[44] E. Dubovik, V. Fridkin, Y.D. Dimos, The bulk photovoltaic effect in ferroelectric $Pb(Zr,Ti)O_3$ thin films, Integr. Ferroelectr. 8 (1995) 285–290.
[45] H. Peelaers, C.G. Van de Walle, Sub-band-gap absorption in Ga_2O_3, Appl. Phys. Lett. 111 (2017) 182104.

[46] V.I. Belinicher, B.I. Sturman, The relation between shift and ballistic currents in the theory of photogalvanic effect, Ferroelectrics 83 (1988) 29–34.
[47] R. von Baltz, W. Kraut, Theory of the bulk photovoltaic effect in pure crystals, Phys. Rev. B 23 (1981) 5590–5596.
[48] S.M. Young, A.M. Rappe, First principles calculation of the shift current photovoltaic effect in ferroelectrics, Phys. Rev. Lett. 109 (2012) 116601.
[49] G. Anoop, et al., Ultra-thin platinum interfacial layer assisted-photovoltaic response of transparent Pb(Zr,Ti)O_3 thin film capacitors, Sol. Energy 111 (2015) 118–124.
[50] P. Zhang, et al., Enhanced photocurrent in Pb($Zr_{0.2}Ti_{0.8}$)O_3 ferroelectric film by artificially introducing asymmetrical interface Schottky barriers, Mater. Chem. Phys. 135 (2012) 304–308.
[51] A. Pérez-Tomás, Functional oxides for photoneuromorphic engineering: toward a solar brain, Advanced Materials Interfaces 6 (2019) 1900471.
[52] J. Robertson, et al., Shallow Pb^{3+} hole traps in lead zirconate titanate ferroelectrics, Appl. Phys. Lett. 63 (1993) 1519–1521.
[53] J. Robertson, W.L. Warren, B.A. Tuttle, Band states and shallow hole traps in Pb(Zr,Ti)O_3 ferroelectrics, J. Appl. Phys. 77 (1995) 3975–3980.
[54] W.L. Warren, et al., Polarization suppression in Pb(Zr,Ti)O_3 thin films, J. Appl. Phys. 77 (1995) 6695–6702.
[55] F. Micheron, Dependence of the photovoltaic effect upon polarization in oxygen octaedra ferroelectrics, Ferroelectrics 21 (1978) 607–609.
[56] A. Pérez-Tomás, M.R. Jennings, M. Davis, J.A. Covington, P.A. Mawby, V. Shah, T. Grasby, Characterization and modeling of n-n Si/SiC heterojunction diodes, J. Appl. Phys. 102 (2007), 014505.
[57] A. Pérez-Tomás, M. Lodzinski, O.J. Guy, M.R. Jennings, M. Placidi, J. Llobet, P.M. Gammon, et al., Si/SiC bonded wafer: a route to carbon free SiO_2 on SiC, Appl. Phys. Lett. 94 (2009) 103510.
[58] Victor E. Henrich, Paul Anthony Cox, The Surface Science of Metal Oxides, Cambridge university press, 1996.
[59] Zhen Zhang, John T. Yates Jr., Band bending in semiconductors: chemical and physical consequences at surfaces and interfaces, Chem. Rev. 112 (2012) 5520–5551.
[60] A. Walsh, K.T. Butler, Prediction of electron energies in metal oxides, Accounts of Chem.Res. 47 (2014) 364–372.
[61] C. Thu, P. Ehrenreich, K.K. Wong, E. Zimmermann, J. Dorman, W. Wang, A. Fakharuddin, et al., Role of the metal-oxide work function on photocurrent generation in hybrid solar cells, Sci. Rep. 8 (2018) 3559.
[62] A. Fontserè, A. Pérez-Tomás, M. Placidi, P. Fernández-Martínez, N. Baron, S. Chenot, Y. Cordier, J.C. Moreno, P.M. Gammon, M.R. Jennings, Temperature dependence of Al/Ti-based Ohmic contact to GaN devices: HEMT and MOSFET, Microelectron. Eng. 88 (2011) 3140–3144.
[63] T. Zhengwei, L. Hong, Z. Fan, J. Tian, L. Zhang, Y. Jiang, Z. Hou, et al., Thinning ferroelectric films for high-efficiency photovoltaics based on the Schottky barrier effect, NPG Asia Mater. 11 (2019) 20.
[64] Lucian Pintilie, Charge transport in ferroelectric thin films, in: Ferroelectrics-Physical Effects, IntechOpen, 2011.
[65] A. Pérez-Tomás, A. Fontserè, M. Placidi, M.R. Jennings, P.M. Gammon, Modelling the metal–semiconductor band structure in implanted ohmic contacts to GaN and SiC, Model. Simul. Mater. Sci. Eng. 21 (2013), 035004.
[66] Simon Sze, Semiconductor Devices: Physics and Technology, John wiley & sons, 2008.
[67] S.L. Mensfoort, M. van, R. Coehoorn, Effect of Gaussian disorder on the voltage dependence of the current density in sandwich-type devices based on organic semiconductors, Phys. Rev. B 78 (2008), 085207.
[68] K. Yao, B.K. Gan, M. Chen, S. Shannigrahi, Large photo-induced voltage in a ferroelectric thin film with in-plane polarization, Appl. Phys. Lett. 87 (2005) 212906.
[69] J.A. Brehm, S.M. Young, F. Zheng, A.M. Rappe, First-principles calculation of the bulk photovoltaic effect in the polar compounds $LiAsS_2$, $LiAsSe_2$, and $NaAsSe_2$, J. Chem. Phys. 141 (2014) 204704.
[70] S. Liu, F. Zheng, A.M. Rappe, Giant bulk photovoltaic effect in vinylene-linked hybrid heterocyclic polymer, J. Phys. Chem. C 121 (2017) 6500–6507.
[71] M. Higashiwaki, H. Gregg, Jessen. Guest Editorial: The dawn of gallium oxide microelectronics, Appl. Phys. Lett. 112 (2018), 060401.
[72] E. Chikoidze, C. Sartel, H. Mohamed, I. Madaci, T. Tchelidze, M. Modreanu, P. Vales-Castro, et al., Enhancing the intrinsic p-type conductivity of the ultra-wide bandgap Gaultra-wide bandgap Ga_2O_3 semiconductor, J. Mater. Chem. C 7 (2019) 10231–10239. https://doi.org/10.1039/C9TC02910A.
[73] S.J. Pearton, F. Ren, M. Tadjer, J. Kim, Perspective: Ga_2O_3 for ultra-high power rectifiers and MOSFETSultra-high power rectifiers and MOSFETS, J. Appl. Phys. 124 (22) (2018) 220901.
[74] S.B. Reese, et al., How much will gallium oxide power electronics cost? Joule 3, 2019, pp. 903–907.
[75] Y.S. Lee, et al., Atomic layer deposited gallium oxide buffer layer enables 1.2 V open-circuit Voltage in cuprous oxide solar cells, Adv. Mater. 26 (27) (2014) 4704–4710.
[76] A. Pérez-Tomas, H. Xie, Z. Wang, H.-S. Kim, I. Shirley, S.-H. Turren-Cruz, A. Morales-Melgares, et al., Pb(ZrTi)O_3 ferroelectric oxide as an electron extraction material for stable halide perovskite solar cells, Sustainable Energy Fuels 3 (2) (2019) 382–389.
[77] C. Li, et al., Positive onset potential and stability of Cu_2O-based photocathodes in water splitting by atomic layer deposition of a Ga_2O_3 buffer layer, Energy Environ. Sci. 8 (5) (2015) 1493–1500.